Probing insulin bioactivity in oral nanoemulsion produced by emulsification assisted electrostatic self assembly cross linking method

Syed Muzammil Munawar[a], Dhandayuthabani Rajendiran[a], Sugantha Kumari Vinoji[b], Khaleel Basha Sabjan[*,c]

[a]*Department of Biochemistry, C. Abdul Hakeem College (Autonomous) Melvisharam 632 509, Ranipet District, TamilNadu, India.*

[b]*Department of Chemistry, Auxilium College, Vellore 632 006, India.*

[*,c]*Department of Chemistry and Biochemistry, C. Abdul Hakeem College (Autonomous) Melvisharam 632 509, Ranipet District, TamilNadu, India.*

Corresponding Author:-

Dr. Khaleel Basha Sabjan

Assistant Professor, Department of Chemistry and Biochemistry, C. Abdul Hakeem College (Autonomous) Melvisharam 632 509, Ranipet District, TamilNadu, India.

Mail id:- khaleelnano@gmail.com

Abstract

This work aimed to develop nanoemulsions coated with nanostarch for oral insulin delivery. Uncoated nanoemulsions were generated by homogenizing water in oil in water (w/o/w) repeated emulsions with castor oil as an emulsifier and span^{TM}-20 as a cosurfactant. The nanoemulsions were prepared by an electrostatic self assembly cross linking technique, yielding a bulk nanoemulsion dispersion containing nanostarch. The coated nanoemulsions had a particle size of around 288±5.11 nm and insulin entrapment efficiency was 99.0%±0.5%. Transmission electron microscopy indicated that the synthesized nanostarch-insulin nanoemulsion was composed of spherical nanoparticles. Circular dichroism spectroscopy revealed insulin's structural stability during preparative stress. An *in-vitro* leakage examination demonstrated that the nanoemulsions remained intact in simulated stomach fluids, phosphate buffer saline and intestinal juices. Normal and diabetic rats both exhibited hypoglycemic symptoms. Furthermore, oral distribution of the coated nanoemulsions had significantly longer hypoglycemic effects than subcutaneous (sc) insulin. The CCK-8 test confirmed the nanostarch-insulin nanoemulsion's safety in human colon adenocarcinoma (Caco-2) cells, and the apparent permeability (P_{app}) of insulin, nanostarch-insulin, was measured. Confocal imaging was used in the colon to confirm enterocyte endocytosis. Finally, the nanoemulsion containing nanostarch-insulin showed prospective delivery system for oral delivery of insulin.

Key words: Oral Insulin, Nanostarch, Caco-2 cells, Nanoemulsion.

1. Introduction

The oral distribution of proteins and peptides has attracted a lot of interest in recent years and new breakthroughs in nanotechnology and biology have opened up new avenues for accomplishing this goal. Among the various peptides and hydrophilic compounds, insulin is the principal peptide for which many respected universities and pharmaceutical companies across the world have aimed for oral delivery. Oral insulin delivery has several significant benefits, including high patient compliance, convenience of administration, and improved patient adherence to medication. More importantly, it is the only route of delivery that may imitate physiological insulin production seen in non-diabetics [1], alleviating patients of hyperinsulinemia and accompanying consequences such as nephropathy and neuropathy. However, oral insulin delivery has two primary bottlenecks, the harsh and deteriorating enzymatic environment of the gastrointestinal tract, which rapidly inactivates insulin, and the mucosal barrier, which lowers insulin's oral bioavailability. Several approaches have been used to bypass the enzyme barrier, with some producing promising results. However, no major progress has been made in addressing the mucosal barrier, which is the primary reason of oral insulin formulation failure. Many smart and difficult ways have been performed to resolve the mucosal barrier, including the application of muco-adhesive nanoparticulate system, muco-adhesive composites, nanoemulsions, double emulsions, chemical alteration of insulin molecules such as acylation and PEGylation to change the hydrophobic/hydrophilic balance of insulin, and the use of cell-penetrating peptides (CPPs) in both chemical and physical conjugation co-administrations. This innovative research study describes a brilliant combination of the most successful and modern approaches to overcoming both the enzymatic state and the mucosal barrier [2]. To overcome the enzyme barrier, insulin was encapsulated and maintained within the polymeric chains of a biodegradable, biocompatible, and muco-adhesive polysaccharide similar to nanostarch, and the tight-junction-opening features of nanostarch-insulin overcame the cell membrane barrier.

Many plants, including cereal grains, vegetables, tubers, and immature fruits, contain starch, a type of storing carbohydrate [3]. Starch is a homopolysaccharide made up of amylase and amylose chains. Amylose is a linear chain of D-glucose units joined by glycosidic α-1,4 bonds. Amylostarch is a branching structure of D-glucose units linked through α-1,4 and α-1,6 linkages. Our research goals were to use the electrostatic self assembly cross linking method to create an insulin-loaded nanostarch-based nanoemulsion with good physical properties for oral delivery, as well as to assess how emulsion droplet size affects the resultant nanoemulsion while probing insulin activity at each step of the process. Nanoemulsions were described in terms of size distribution, surface charge, form, EE, and *in-vitro* insulin release behaviour, with insulin activity assessed during and after each stage of processing, either *in-vitro* or *in-vivo*. The goal of our study was to create a nanostarch-based nanoemulsion for oral insulin administration as a model pharmaceutical. The primary limitation of emulsion systems is thermodynamic instability, which can be solved by adjusting parameters such as efficient emulsifiers. Emulsifiers affect the size distribution of droplets, the zeta potential, optical and physical properties, encapsulation efficiency, and stability. As a result, selecting the right emulsifier for creating optimized emulsions is critical.

2. Materials & Methods

2.1 Materials

All analytical-grade chemicals were used in our research study. Starch low molecular weight, Monobasic sodium phosphate, Dibasic sodium phosphate, Span^{TM}20, Glycerol, were purchased from Sigma Aldrich. Castor oil was supplied by Sigma-Aldrich Mumbai. Insulin, Biphasic isophane, (40 I.U/ml, 10 ml), [(Human Mixtard, Monocomponent Biosynthetic *r*-DNA insulin obtained from Torrent Pharmaceuticals Ltd), (Novo Nordisk India Pvt Ltd)]. Caco-2 (human epithelial colorectal adenocarcinoma cell) was purchased from American Type Culture Collection (ATCC) (Rockville, MD, USA). For all the experiments, milli-Q deionized water was used. All other chemicals used were of Good and Analytical grade.

2.2 Preparation of Nanostarch

Nanostarch was prepared by acid hydrolysis of starch according to the method by [4], with minor modification. Starch powders (50 g) were mixed with 500 mL of 3.16 M H_2SO_4 solution and placed at 40^{o}C for 3 and 7 days under stirring at the speed of 200rpm. For the Hydrochloric acid hydrolyzed starch, 20 grams starch powders were mixed with 400mL (2.2-N HCl) hydrochloric acid solution at 40^{o}C for 7 days with constantly stirring at the speed of 200 rpm. The suspensions were washed by successive centrifugations in milli-Q deionized water until pH 7 was constant. The resultant suspensions were re-dispersed using Ultra Turrax T20 (IKA) at 13,500 rpm for 3 minutes to avoid aggregates and stored at 4^{o}C with several drops of chloroform. The NS concentrations were determined by weighting freeze-dried powders of the homogeneous dispersion of NS (10 ml) and expressed as weight percentage relative to the volume of the water phase. The concentrations of H_2SO_4 and HCl-hydrolyzed NS suspensions were 3.00% (w/v) and 2.00% (w/v) respectively. Different concentrations of NS suspensions were derived by diluting the stock homogeneous dispersion of NS.

2.3 Preparation of Nanostarch/Insulin-coated nanoemulsion

A two-step process was employed to prepare the o/w emulsion [5]. Briefly, the o/w primary emulsion was formed by preparing 800 µL Insulin solution, 150 mg insulin dispersed in 10 mL phosphate buffer solution (PBS, 0.2 M) at pH 7.4 (USP 34) and added to 8 g of the oily phase composed of castor oil as surfactant, span^{TM}-20 as cosurfactant with stirring for 15 minutes at 800 rpm. Insulin-loaded nanoemulsions were prepared through a modified emulsification electrostatic self assembly technology. Then this primary emulsion was dropped into above prepared nanostarch, at various concentrations ratios (1:1, 1:3, 3:3). The so formed nanoemulsion after continuous stirring at 600 rpm for 15 minutes. This optimization and optimized formed nanoemulsion ratio 3:3 was selected for the further studies.

3. Determination of entrapment efficiency

Following the destruction of the coated nanoemulsion, the leakage ratio was used to calculate the entrapment ratio (ER). Briefly, 1mL of nanoemulsion was dissolved in 4mL of methanol [6]. After vigorously mixing in 100 µL of HCl (pH 1.0), the pH reached 3.0, milli Q water was added to make 10 mL and then thoroughly mixed. After spinning at 16000 g for 10 minutes, the clear supernatant was tested for insulin using HPLC.

Permeation assays were performed in identical amounts of isotonic calcium chloride 204 mEq/L, pH 7.4 solutions to determine the influence of calcium binding on intestinal permeability. At ½ hour, 1 hour, 2 hours, 3 hours, 4 hours, 5 hours, 6 hours, 7 hours, and 8 hours, an aliquot of 1 mL of medium was withdrawn from the receptor tube and replaced with an equivalent volume of new medium. The insulin content of the samples was determined with a previously reported HPLC technique. An analogous work on insulin solution is currently being reviewed. The amount of insulin encapsulated in the nanoemulsion was calculated as the difference between the total amount employed in the formulation and the amount of free insulin left in the outer aqueous phase after centrifugation.

$$\text{EE (\%)} = \frac{The\ total\ amount\ of\ Insulin - Amount\ of\ free\ Insulin\ in\ the\ Supernatant}{The\ total\ amount\ of\ Insulin\ added} \times 100$$

4. Determination of insulin

Insulin levels were determined using a reversed-phase HPLC ultraviolet (UV) technique [7]. The HPLC system (1100 series, Agilent Technologies, Santa Clara, CA, USA) consisted of a quaternary pump, a degasser, an auto-sampler, a column heater, and a tunable UV detector. A C18 column Zorbax, 5 m, 4.6 mm 150 mm, Agilent, and a C18 pre-column 2 mm 20 minutes, Alltech, were utilized for detection at 25°C. The mobile phase consisted of acetonitrile and 0.57% phosphoric acid solution adjusted to pH 2.25 with triethylamine in a volume ratio of 26:74. The detection wavelength was λmax 220 nm and the flow rate was set to 1.0 mL/min.

5. Characterization of coated and uncoated nanoemulsion

5.1 Size and zeta potential

The average particle size and size distribution of the nanoemulsions were assessed using dynamic light scattering (DLS) on a NICOMP 380 DLS device (Santa Barbara, CA, USA). Before measurement, the nanoemulsion was 500 times diluted in deionized water [8]. At 25°C, the zeta potential was determined using a Zetasizer Nano ZS (Malvern Instruments, Malvern, UK). Samples were collected using foldable capillary cells equipped with gold electrodes. Three measurements were obtained, and the software automatically determined the number of runs for each. The data were provided as mean standard deviation (SD).

5.2 Physical stability of nanoemulsion

The stability of the produced nanoemulsions was assessed using the centrifugal acceleration method. A 5 mL Eppendorf tube was filled with 4 mL of nanoemulsion, which was then spun at 3000 g for 10 minutes in a desktop centrifuge (Anke TGL-16G, Shanghai). A 0.8 mL sample of subnatant was softly and steadily pipetted from the tube's bottom. The samples were then vortexed for 20 seconds before being transferred to a 50 mL volumetric flask and diluted with milliQ water to achieve the necessary final volume. At λmax 500 nm, the absorbance of diluted nanoemulsions was determined spectrophotometrically [9]. The centrifugal stability constant (K_e) was derived using this method.

$$ke = \frac{A_0 - A}{A_0} \times 100\%$$

where A_0 and A are the absorbance of the diluted nanoemulsion before and after centrifugation, respectively.

5.3 Transmission electron microscopy (TEM)

Transmission electron microscopy was utilized to investigate the morphologies of uncoated and nanopectin-insulin nanoemulsions (coated). A drop of nanoemulsion was applied on 300-mesh carbon-coated copper grids, and any excess water was wiped off with blotting paper [10]. Before drying at room temperature, the stain was treated with a 60-second drop of 1% phosphotungstic acid. The samples were tested at an acceleration voltage of 120 kV. The pictures were collected at a final magnification of 12,000 times.

5.4 Conformational stability of insulin

The conformational stability of insulin was determined using circular dichroism (CD) spectroscopy (Jasco J-810; Jasco Corp, Tokyo, Japan). The coated nanoemulsion of 1 mL was destroyed by combining 4 mL of methanol and a pH 1.0 hydrochloric acid solution in 10 mL. After 10 minutes of centrifugation at 16,000 g, insulin was extracted from the supernatant [11]. Following that, the insulin was separated using a Supelco ENVI-18 solid-phase extraction column (Sigma-Aldrich). To summarize, the ENVI-18 column was activated using methanol before being balanced with a solvent. The supernatant mixture (1mL) was then plated. Impurities were removed with 3 mL of 40% aqueous methanol before eluting the insulin with 30 mL of 60% aqueous methanol. To perform the circular dichroism test, a hydrochloric acid solution was used to increase the insulin concentration to 30 µg/mL. At 20°C, spectra were obtained with a 0.5 nm step size, a maximum λmax range of 200-300 nm, a band width of 3 nm, a scanning speed of 500 nm/min, and a reaction time of 0.25 seconds. The Jasco w32 secondary structure estimate software version 1.0 was used to calculate secondary structure content.

5.5 *In-vitro* drug release

The rate and extent of insulin release as a model drug were investigated in both simulated intestinal fluid (SIF, pH 6.8, duodenum pH) and phosphate-buffered saline (PBS, pH 7.4, colon pH) to assess the viability of the suggested delivery mechanism for peptide and protein oral delivery [12]. To test the *in-vitro* release of insulin from carbohydrate-like nanostarch, 30 mg of lyophilized nanoemulsion was combined with 500 mL of SIF solution and shaken at 50 rpm. The temperature remained at 37°C±5°C. To achieve the sink condition, the releasing medium was designed to be quite large. At specified intervals, 1 mL aliquots were drawn and replaced with preheated blank media. For 20 minutes, the samples were centrifuged at 14,000 rpm. Instead of adding blank medium following aliquot withdrawal, the supernatant was analysed for insulin concentration, and the sediment was dispersed in 1 mL blank media before reintroducing it into the release medium because the insulin release from the nanoemulsion's polymeric mesh did not finish within the first few hours, the remaining insulin in the withdrawn nanoemulsion was also released. The insulin concentration in the supernatant was determined using a previously described HPLC procedure. To further understand the process of peptide release from the nanoparticulate drug delivery device, *in-vitro* insulin release data was fitted to the Ritger-Peppas equation.

$$\frac{M_t}{M_\infty} = Kt^n$$

Mt and M∞ denote cumulative insulin release at time (t) and infinite time, respectively. K is a constant related to the device's structural and geometric properties, while 'n' is an exponent reflecting the diffusion mechanism. The number of calculated values for 'n' was used to find the release mechanism. If n = 0.45, the release mechanism is Fickian/case I diffusion, 0.45 < n < 0.89, non-Fickian/anomalous transport; and n = 0.89, diffusion and zero-order (case II) transport.

5.6 *In-vitro* cytotoxicity of nanoemulsions

Caco-2 cells grow under high glucose conditions. Dulbecco's modified Eagle medium has 10% foetal bovine serum, 1% v/v non-essential amino acids, 50 U/mL penicillin, and 50 µg/mL streptomycin. Caco-2 cells were cultivated as monolayers for 21 days [13]. Cells were grown at 37°C in 5% CO_2 in a culture medium that was changed every two days for the first 15 days and daily for the last week. Over a 24-hour period, the MTT test was used to assess the cytotoxicity of a nanostarch-insulin nanoemulsion on Caco-2 cells. Caco-2 cells ($1x10^5$ cells/well) were grown in 6-well plates for 24 hours before being covered with sterile glass cover slips to allow for confocal microscopy imaging. At staggered time intervals, the cells were treated with insulin-FITC and insulin-FITC loaded nanostarch-insulin nanoemulsion at 10 µg/mL concentrations. Cell monolayers were properly cleansed with PBS pH 7.4 before being examined under a confocal microscope (CLSM, Carl Zeiss Microscopy GmbH, Germany). Individually seeded Caco-2 cells were treated with the endocytic inhibitors chlorpromazine HCl (5 µg/mL), nystatin (50 µg/mL), amiloride (13.3 µg/mL), and colchicine (10 µM) for 1 hour at 37°C. Caco-2 cells were grown with heparinases (5U) to evaluate the adsorptive absorption mechanism. Pretreatment of cells with a 1 mM folic acid solution inhibited receptor-mediated endocytosis. The cells were subsequently incubated with a nanostarch-insulin nanoemulsion containing 10 µg/mL insulin for four hours at 37°C. Before being lysed with 0.1% Triton X-100, the cells were washed three times in cold PBS. In the absence of inhibitors, the manufacturer recommended ELISA kit was utilised as a control to determine intracellular insulin absorption.

5.7 Transepithelial electrical resistance (TEER) and insulin transport studies

Caco-2 cell lines were grown in transmembrane inserts with 0.4 µm pore size (Millipore) and 5×10^5 cell density per well. TEER investigations were carried out utilising a previously disclosed methodology. The TEER of the cell monolayer was determined at defined time intervals at 37°C using either plain nanostarch nanoemulsion or nanostarch-insulin loaded nanoemulsion at a concentration of 10 mg/mL/well. According to some studies [14], aspart insulin, a novel and short-acting analogue of human insulin, was also loaded at the same concentration into either plain nanostarch or nanostarch-insulin loaded nanoemulsion. Aspart insulin has a better ability to pass through the lumen epithelium due to its monomeric nature and linear shape in aqueous medium. We examined human insulin and aspart insulin (Alpha Diagnostic International) under identical settings and compared the results to see whether our nanoparticulate approach outperformed aspart insulin. As a control, a simple solution comprising both human and aspart insulin was injected into the cell layer's donor chamber. For insulin transport studies, the donor chamber medium was replaced with new media containing insulin-loaded plain nanostarch or nanostarch-insulin nanoemulsion (10mg/well).

Aliquots from the receiver chamber were collected at predefined time intervals over a 4-hour period, and the insulin content was measured using a proprietary ELISA kit that was specific to and sensitive to both conventional human insulin and aspart insulin. The average results for all instances assessed in triplicate were presented. The apparent permeability coefficient (P_{app}) of insulin was calculated using the following equation. In this equation, dQ/dt indicates the permeability rate, A is the filter membrane's surface area, and C_0 is the starting insulin concentration in the apical chamber.

$$Papp = \frac{\frac{dQ}{dt}}{A \times C_0}$$

5.8 Pharmacokinetics study

The animal procedure was authorised by the institution's ethical committee. Male albino wistar rats, weighing 180g±10% and aged 2-3 months, were maintained in room temperature plastic cages with a 12-hour light/dark cycle. They were given rat feed and unfettered access to water. The CSLM method was utilized to imitate the intestinal absorption and localization of an insulin-FITC solution and a nanostarch-insulin nanoemulsion with 10 µg/mL insulin. Male albino rats were given a single intraperitoneal injection of 60 mg/kg streptozotocin to induce diabetes. The diabetic rats in the study had blood glucose levels that exceeded 250 mg/dL. Thirty diabetic rats (n=6) were split into five groups. The glucose levels in rat blood were measured using a colorimetric glucose assay kit (Cell Biolabs, Inc., USA). At various time intervals, the percentage drop from the starting value was determined. The total drop in blood glucose level (TD%) was estimated using the equation below [15].

$$TD\% = \frac{AUEC_c - AUEC_s}{AUEC_c}$$

where $AUEC_c$ represents the area beneath the curve after oral administration of PBS to diabetic rats/control diabetic, and $AUEC_s$ represents the area beneath the curve after oral administration of nanostarch-insulin nanoemulsion and insulin SC injection, respectively. In groups 1 and 3, plasma insulin levels were determined with an ELISA, and the pharmacokinetic parameters C_{max}, T_{max}, AUC, mean residence time (MRT), and relative bioavailability (F%) were examined.

6. Statistical Data Analysis

The findings were presented as the mean and standard deviation. A one-way analysis of variance was used to compare groups (SPSS 16.0, IBM Corp, Amonk, NY). A difference was judged statistically significant when the *P*-value was less than 0.05.

7. Results & Discussions

7.1 Insulin Encapsulation efficiency

The insulin encapsulation efficiency was around 99.0% ± 0.5%. The high level is due to the pH influence of nanoemulsion components. Insulin's isoelectric point is approximately pH 5.3, but starch's pKa values range from 3.0 to 4.0. As a result, at a final pH of 4.0, strong electrostatic self assembly attractions may occur, resulting in a high EE for the negatively charged protein [16].

Furthermore, calcium ions bind with nanostarch residues, generating electrostatic bridges with insulin's negatively charged carboxylic acids, so enhancing the contact between the two. The use of emulsifiers like castor oil and cosurfactants like span20 can also boost insulin encapsulation efficiency due to the emulsifier's molecular steric stability.

7.2 Zeta potential

The electrostatic self assembly cross linking technology was used to produce a simple and dependable nanostarch/insulin-coated nanoemulsion in a 3:3 ratio. Starch's surface net charge remained positive at pH >4.0 (ζ-potential +19.80±1.60 mV). The ζ-potential is the electrical potential at the hydrodynamic shear plane relative to the solvent. Our study utilized ζ-potential to determine the charge state of polyelectrolytes at a specific working pH. Abodinar *et al.*, studied the conformation and chain flexibility of polyelectrolytes in dilute solution, as well as their ionic strength dependency, using -potential measurements to determine ionic strength [16]. The ζ-potential parameter is not a substitute for potentiometric or conductimetric research due to its sensitivity to polyelectrolyte structural and conformational properties. At pH <4.0, starch's amphiphilic capacity reduces due to dissociation of various groups in its structure. Any polymeric nanoparticulate delivery system intended for oral peptide delivery, such as Insulin, must meet certain basic requirements, including appropriate Insulin encapsulation, high drug encapsulation efficiency, and drug loading efficiency. As a result, even when an appropriate and realistic amount of polymeric nanoemulsion is supplied orally, low insulin EE precludes the nanoparticulate delivery method from achieving the required therapeutic benefits. Submicron carriers have previously been used to demonstrate insulin absorption across intestinal membranes. The impact of nanoemulsion size is obvious, as larger particles are more likely to remain in the Peyer's patches, which are densely packed with M-cells, resulting in slower activity. Smaller nanoemulsions, if properly charged, can bypass the lymphatic system and enter the systemic circulation. M-cells prefer nanoemulsions smaller than 1 μm, namely 200 nm or less. As a result, the first step in our study was to shrink the w/o/w emulsion droplets to nanoscale size. Calcium is required for strong intestinal connections and membrane integrity. To recap, the nanoemulsion's potential to improve mucosal transport is advantageous. Tight connections can also be opened to compensate for cell shrinkage caused by nanostarch's increased ability to absorb water. The capacity of the nanostarch-insulin nanoemulsion to tolerate gastrointestinal enzymatic breakdown is an essential factor in determining oral insulin bioavailability. There was no significant difference in particle size or zeta potential in the presence of pepsin, trypsin, or chymotrypsin (Graph 1), and the nanostarch-insulin nanoemulsion preserved more than 82% of the entrapped / encapsulated insulin in the three different biological enzymes. Under the same conditions, more than 85% of naked insulin was destroyed. The capacity of the nanostarch-insulin nanoemulsion to withstand extreme gastrointestinal conditions could be ascribed to nanostarch carboxylic / amino groups that bind with Ca^{2++}, a known cofactor for enzyme performance. Finally, there were no significant changes ($p > 0.05$) in EE%, particle size, or zeta potential at different time intervals (Table 1) or after 6-month storage at 5°C, indicating the insulin nanoemulsion's physical durability.

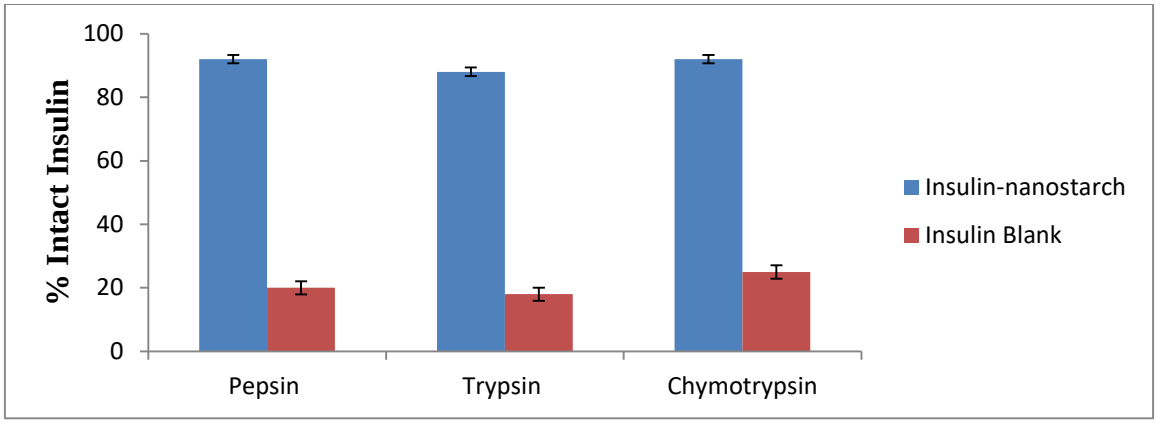

Graph 1 Effect on entrapment efficiency

Under controlled conditions, the carboxylate groups in starch were expected to interact electrostatically with oppositely charged groups in insulin, resulting in the development of a stable nanoemulsion by electrostatic self-assembly cross linking. The ζ-potential of the nanoemulsion is proportional to the surface charge density values due to the electrostatic self-assembly of nanostarch and insulin. The particle size measured was 288±5.11 nm (Fig. 1a,1b), and the average Zeta potential (ζ) was +19.80±1.60 mV (Table 1). Encapsulation with nanostarch-insulin nanoemulsion resulted in a considerable decrease in [17]. At gut pH, the carboxyl groups on nanostarch may have carried a negative charge, enhancing its propensity to chelate cations such as calcium and dissociating the starch structure's carboxylic groups a crucial co-factor for proteolytic enzymes that limits their activity. Ca^{2+} binding empathy has also been shown to disrupt cellular actin and adherents, activate protein kinases, and thereby open tight junctions. Transmission electron micrographs reveal that nanoemulsions are smooth, with no cracks or pores (Fig. 1b). Finally, the insulin nanoemulsion's physical stability was proven by the absence of significant changes ($p > 0.05$) in EE%, particle size, and zeta potential throughout time and after 6-month storage at 5°C (Table 1).

7.3 Physical stability

Nanoemulsion bioavailability is mostly determined by particle size, dispersion, and physical stability. In this investigation, we looked at how homogenization, sonication, insulin peptide concentration, w/o/w ratio, and pH influenced particle size, polydispersity index (PI), and physical stability of nanoemulsions [17].

7.4 Morphology of the coated nanoemulsion

The TEM picture had a size of approximately 288±5.11 nm, which fits dynamic light scattering measurements of 250.0 nm (Polydispersion Index [PI] = 0.29) for uncoated nanoemulsions and 200-400 nm (PI = 0.211±0.014) for coated nanoemulsions. The uncoated nanoemulsion droplets had a nearly round shape and a smooth profile (Fig 1a, 1b). However, the nanoemulsion covering had a rough and uneven appearance [18]. This experience is consistent with the accounts of others. The cross-linking of nanostarch and protein may have altered surface tension, resulting in surface shrinkage and reduced particle size in nanoemulsions.

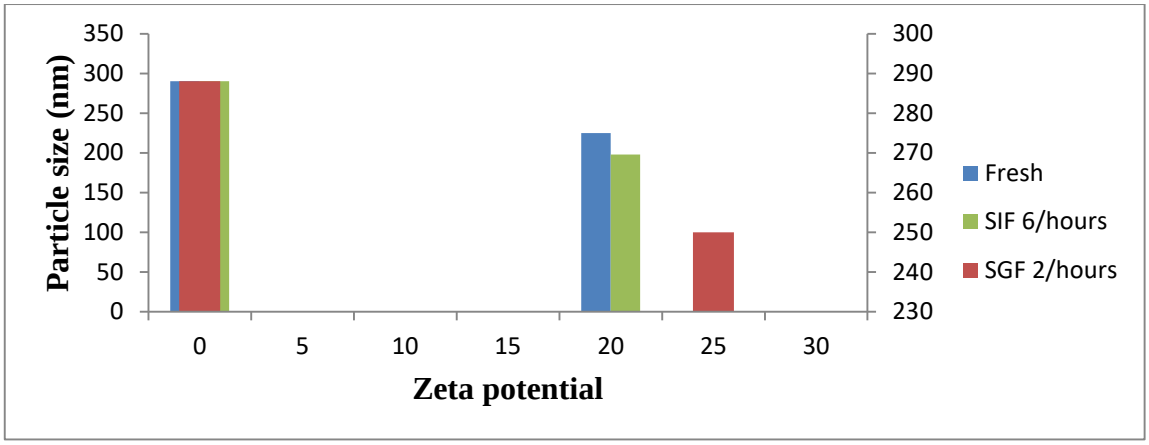

Graph 2 Effect on particle size and zeta potential

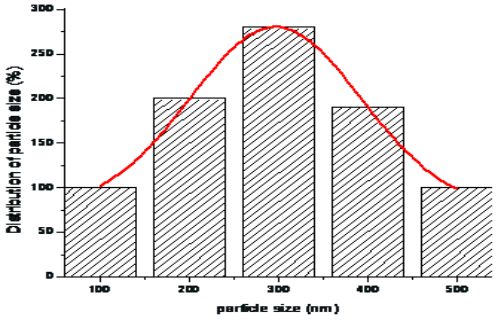

Figure 1a Histogram of nanoemulsion

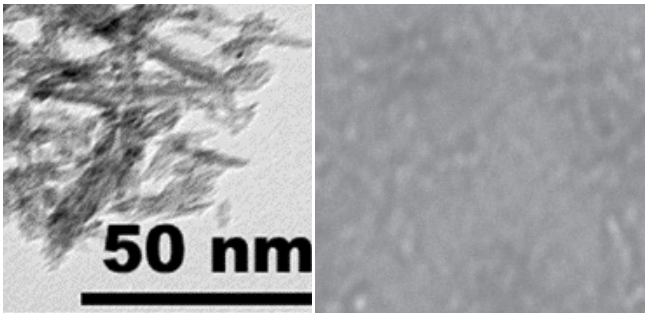

Figure 1b TEM of uncoated and coated nanoemulsion

Table 1 Physico-chemical Characterization of insulin-nanostarch nanoemulsion

Parameter	Particle size (nm)	PDI	Zeta potential	Calcium binding efficiency*
Result ± SD	288 ± 5.11	0.29	+19.80±1.60 mV	25.00 ± 2.00

Results are mean of three replicates ± standard deviation. *Data were presented as % to the initial calcium concentration.

7.5 Conformational stability of insulin

Particle size and dispersion, as well as physical stability, are widely recognised as essential factors influencing nanoemulsion bioavailability. In this study, we investigated how the oil-to-water ratio and pH influenced particle size, polydispersity index (PDI), calcium binding efficacy, and physical stability of nanoemulsion. High temperatures, mechanical manipulation, and exposure to organic solvents can all degrade protein/peptide structure, which is necessary for good therapeutic efficacy. As a result, when altering proteins or peptides, conformational stability needs to be considered. Circular dichroism spectroscopy evaluates protein and peptide secondary structures, including α-helix and β-fold, to assess insulin effectiveness [19]. Circular dichroism is an example of dichroism. Figure 2 depicts the spectroscopic spectra of insulin secondary structures.

The spectra of insulin combined with nanoemulsion and coated nanoemulsion were identical to those of insulin solution, with a peak valley of 209 nm and a shoulder of 225 nm. Insulin secondary structures remained constant across samples (21-22% α-helix and 27%-29% β-folds). This secondary structural investigation demonstrates that insulin's conformational shape remained unchanged during the production of nanostarch-insulin coated nanoemulsions.

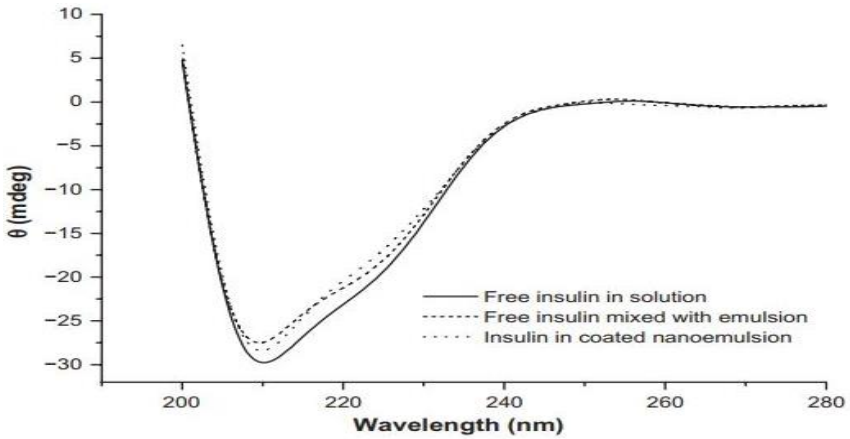

Figure 2 Circular dichroism spectrascopy of nanoemulsion

7.6 *In-vitro* release study

Graph 2 shows the *in-vitro* release curve of model peptide insulin from an optimised nanoemulsion delivery device loaded with the embedded peptide during a post-loading operation [20]. The release profile was assessed at SIF pH 6.8, SGF pH 1.2, and phosphate-buffered saline pH 7.4. Both media demonstrated a spike of insulin release during the first 30 minutes, which thereafter decreased but remained constant over the next 24 hours. During the burst release phase, almost 33%±6% of total insulin is released at pH 7.4, 20%±2.1% at pH 6.8, and 22%±2.3% at pH 1.2.

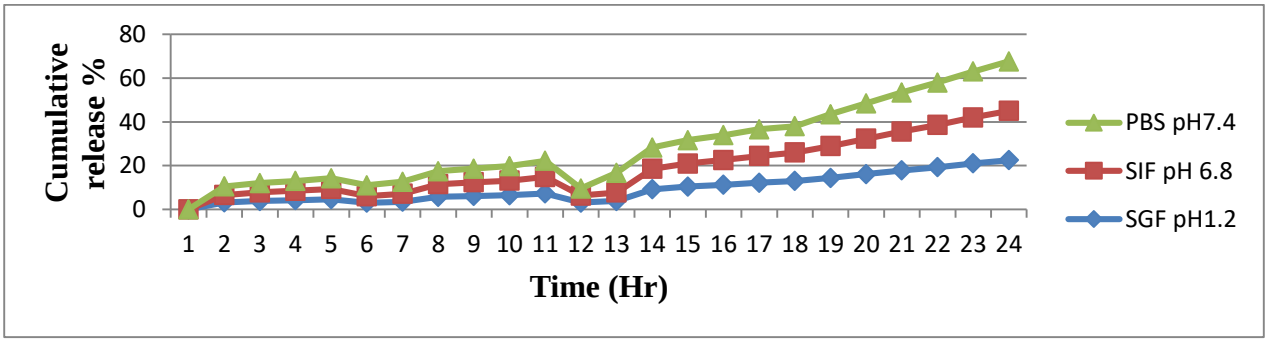

Graph 3 Nanostarch-Insulin release profile from PBS pH 7.4, SIF pH6.8, and SGF pH1.2

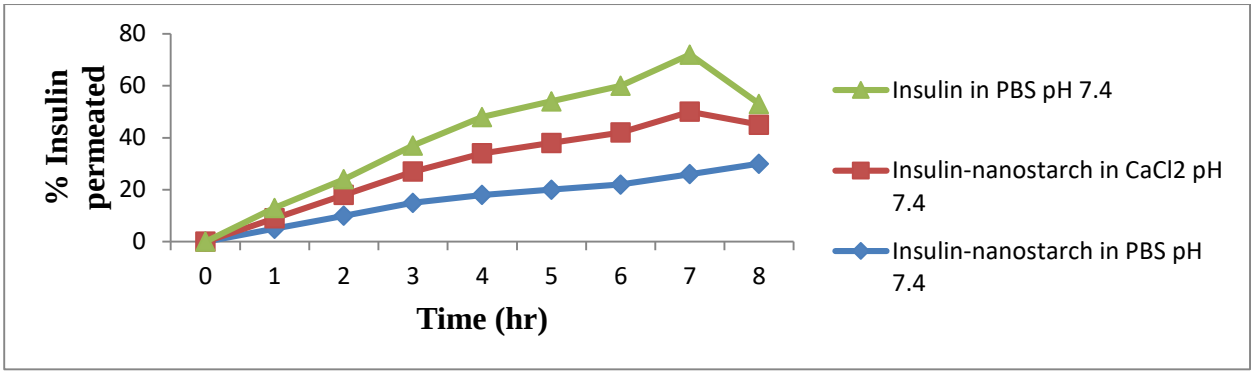

Graph 4 Insulin permeability in the rat gut and the influence of several stomach enzymes

During optimisation testing, we discovered that nanoemulsions with specific polysaccharide and emulsifier-cosurfactant concentrations had the maximum loading efficiency, release behaviour, and total release extent. Graph 3 demonstrates that insulin release from the optimised nanoemulsion was nearly complete after 24 hours, with 86% of the implanted insulin released in phosphate-buffered saline pH 7.4 at this point. Burst and total insulin release were lower in SIF pH 6.8, 1.2, and phosphate-buffered medium, with 20%±2.1% burst release and 78%±6.5% total release in SIF pH 6.8 and 1.2, respectively. At pH 6.8, several of nanostarch's primary carboxy groups may still be protonated, retaining cationic charges [21], attracting negatively charged insulin and delaying release. At pH 7.4, this formulation demonstrated extremely high burst and total release. Graph 4 shows the influence of various stomach enzymes on *ex-vivo* insulin permeability in the rat gut. Because of its amphiphilic properties, the polysaccharide in this formulation is water soluble at all pH levels. Aside from normal solubility, the polysaccharide's cationic charge may have been lost at this pH, preventing it from binding to and retaining negatively charged insulin. This rapid peptide release from the nanoemulsion's polymeric mesh is beneficial for peptides with short half-lives, such as insulin, because it enables the delivery mechanism to maintain therapeutic advantages. Another study discovered that the mechanism of drug release from erodible, hydrophilic polymer matrices is a complex process involving a number of factors, including water penetration into the polymeric matrix, solubilization / erosion of the polymeric formulation, polymer swelling, and drug dissolution from the enlarged matrix. Drug release from polymeric formulations with swelling properties is usually non-Fickian / anomalous; but, for large molecules like peptides and proteins, the situation can change, especially when ionic charges interact between the carrier polymer and the enclosed moiety. To explore the release mechanism of insulin as an ionic charge peptide from the synthesised and produced nanoemulsion, the parameter "*n*" for the Ritger-Peppas equation was calculated. The optimised formulation resulted in a correlation coefficient of 0.8213 ($R \geq 0.99$), confirming that the release data fits the empirical equation. The "*n*" release exponent varied from 0.86 to 0.89, indicating non-Fickian or anomalous transport ($0.45<n<0.89$).

7.7 Transepithelial electrical resistance (TEER) and insulin transport studies

MTT cytotoxicity tests revealed that both uncoated nanostarch and coated/encapsulated nanostarch-insulin had no effect on Caco-2 cell lines *in-vitro*. The particles had nearly 100% cell viability as compared to the control media.

Graph 5 shows that after 2 hours of exposure to Caco-2 cells with either uncoated or coated/encapsulated nanostarch-insulin at a dose of 10 mg/mL/well, there was a significant reduction in TEER of ~86 and 41%, respectively, compared to the initial values of coated/encapsulated and uncoated nanostarch. TEER values were significantly lower in the presence of both native coated and uncoated nanoemulsions, regardless of whether the embedded peptide was regular human insulin or aspart insulin, but there was no significant difference in the presence of a simple solution of regular human insulin or aspart insulin. The presence of nanstarch nanoemulsion reduces TEER, a well-established scientific fact validated by several investigations. Our findings, however, revealed a considerable and dramatic difference in TEER reduction between uncoated and coated nanostarch nanoemulsions. Graph 3 demonstrates that the TEER reduction in the presence of coated encapsulated nanostarch-insulin was more than double that of the uncoated nanostarch nanoemulsion.

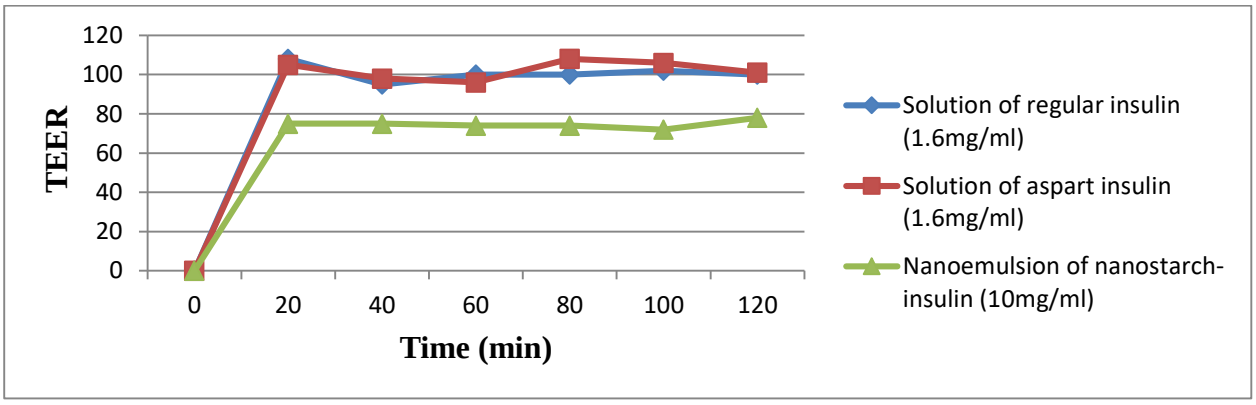

Graph 5 Outcome of diverse formulations on TEER

The concentration of insulin in transwell receptor chamber samples was determined with an ELISA kit developed for conventional human insulin and aspart insulin. Calculating the cumulative transferred insulin in the receiver chamber and comparing it to the initial concentration of insulin in the donor chamber revealed that insulin translocation across the cell monolayer was ~0% for simple solutions of ordinary or aspart insulin. The yield of standard nanostarch nanoemulsion loaded with typical human insulin is around 6%, while aspart insulin yields 6.5%. Coated nanostarch-insulin nanoemulsion loaded with standard human insulin yields around 19%, whereas aspart insulin delivers approximately 17.8%. This is the highest level of insulin translocation from the donor side of Caco-2 cells seen in cell culture research thus far. Graph 3 depicts the aggregate transit of different insulins. Our findings, as well as release testing, demonstrate that the nanoparticulate nanoemulsion system and its unique properties, rather than the type of insulin, impact how much insulin is delivered across the cell monolayer. Our results contradict another study's suggestion that aspart insulin is easier to inject orally due to its monomeric nature. Another fascinating finding in this study is that inhibiting insulin translocation by extracting insulin-containing samples from the receiver chamber and incubating them in fresh micro tubs for 24 hours raises the concentration of assayable insulin over time.

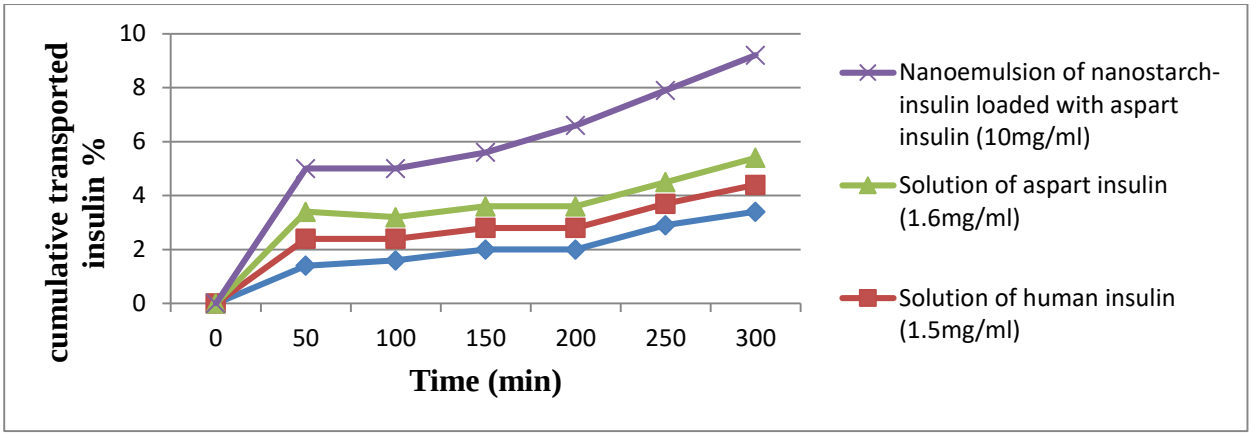

Graph 6 Collective transported formulation of insulin

Our findings are consistent with *in-vitro* release investigations, which indicate that insulin release is essentially complete after 24 hours (Graph 6). As a result, it is assumed that a greater proportion of insulin is translocated *via* nanoemulsion translocation, that numerous embedded insulin molecules are translocated from the apical to the basolateral chamber with each nanoemulsion translocation, and that insulin release from nanostarch-insulin coated nanoemulsion will persist. As previously stated, this prefabricated nanoparticulate nanoemulsion system may be simply loaded with a huge number of peptides, proteins, nucleotides, and other big and hydrophilic molecules in a simple and modest post-loading process because of nanoparticulate properties such as muco-adhesion and tight-junction opening properties of nanostarch, as well as direct and energy-independent [22], penetration potential of nanostarch-insulin, the embedded peptide will be translocated after the nanostarch-insulin coated nanoemulsion is exposed to biological barriers. The effect of nanoemulsion size is clear, as larger particles are more likely to reside in Peyer's patches, which are densely packed with M-cells and so have slower activity. Smaller nanoemulsions can cross the lymphatic route and enter the systemic circulation if properly charged. The findings indicate that this delivery approach was meticulously devised, taking use of the incredible tight-junction opening and unique cell penetration potentials of cell penetrating peptides. This nanoemulsion nanoparticulate system appears to have considerable potential for noninvasive administration of peptides, proteins, vaccines, and nucleotides, as well as drug delivery to the blood-brain barrier and distribution of diagnostic and contrast media from blood-brain barrier compartments.

7.8 *In-vitro* cytotoxicity assessment

Cell viability was above 90% at doses similar to 10 µg/mL insulin (Fig. 3a-3f). Higher insulin nanoemulsion concentrations dramatically reduced cell viability ($p<0.05$), potentially due to higher nanostarch content. In general, the nanoemulsion's moderate positive charge value improves its safety [23]. In following tests, a nanostarch-insulin nanoemulsion containing insulin at a concentration of 10 µg/mL was used.

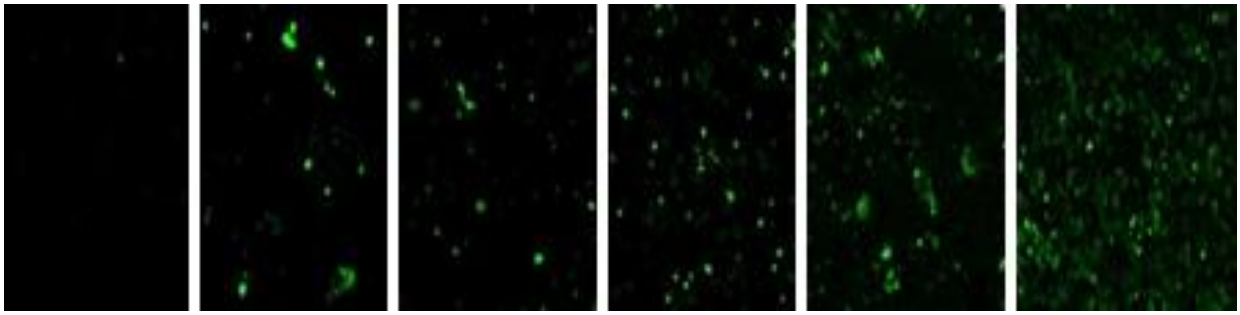

(a) (b) (c) (d) (e) (f)

Figure 3 Images of Light microscope as Caco-2 exposure to (a) insulin-FITC for 5 hr, nanostarch-insulin for 1,2,3,4 and 5 hours

7.9 *In-vitro* Caco-2 cellular uptake

Caco-2 cells produced no fluorescence after 5 hours of insulin-FITC incubation (Figs. 3a-3f). Insulin's high molecular weight prevents cellular internalisation [24]. In contrast, CLSM micrographs of a nanostarch-insulin nanoemulsion revealed a high number of green fluorescent spherical particles, indicating insulin cellular internalisation. Furthermore, the intensity of the fluorescent dye increases with incubation time.

7.10 Tracking the nanostarch-insulin nanoemulsion cellular uptake pathway

Figure 4a-4c shows the outcomes of this experiment nanostarch decreased insulin absorption in Caco-2 cells ($p<0.05$), indicating that the nanostarch-insulin nanoemulsion enhances insulin internalisation [25]. To determine the mechanism of nanoparticle uptake, Caco-2 cells were pre-treated with chlorpromazine, nystatin, amiloride, and colchicine, which caused clathrin-mediated endocytosis, caveolae-mediated endocytosis, macropinocytosis, and microtubular-mediated endocytosis, respectively. Except for chlorpromazine, all inhibitors significantly reduced cellular internalisation of insulin nanoparticles ($p>0.05$), indicating that insulin-Nanostarch nanoemulsion does not require clathrin-mediated endocytosis for transport. Nystatin, on the other hand, is a cholesterol-binding agent that prevents sag formation and thus caveolae-mediated endocytosis. Previous research has revealed that caveolae-mediated endocytosis entails detaching caveolae from the plasma membrane in order to transport nanocargo to caveosomes while avoiding the degradative lysosomal route. Amiloride also inhibits macropinocytosis by blocking Na^+/H^+ exchange in the plasma membrane, which is required for the process. Colchicine suppresses microtubule polymerization by binding irreversibly to tubulin, which reduces microtubule-mediated endocytosis. Microtubules, in general, form a cytoplasmic network that aids in endocytic vesicle trafficking. The presence of heparan sulphate proteoglycans results in a negatively charged cell membrane. Heparinases are enzymes that hydrolyze different proteoglycans found on cell membranes, thereby mitigating their detrimental effects. Enzyme pre-treatment of Caco-2 cells reduced insulin cellular internalisation by 80% due to a decrease in electrostatic contact between the less negative cell membrane and the cationic nanoparticles. Finally, by targeting Vitamin B_{12} receptors, the particles are supplied by non-destructive caveolae-mediated endocytosis.

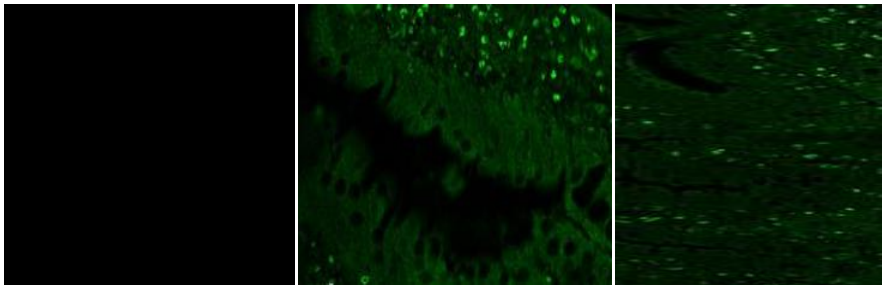

(a) (b) (c)

Figure 4 Confocal (CS) of rat intestinal mucosa and orally (a) insulin-FITC (b), and (c) nanostarch-insulin-FITC

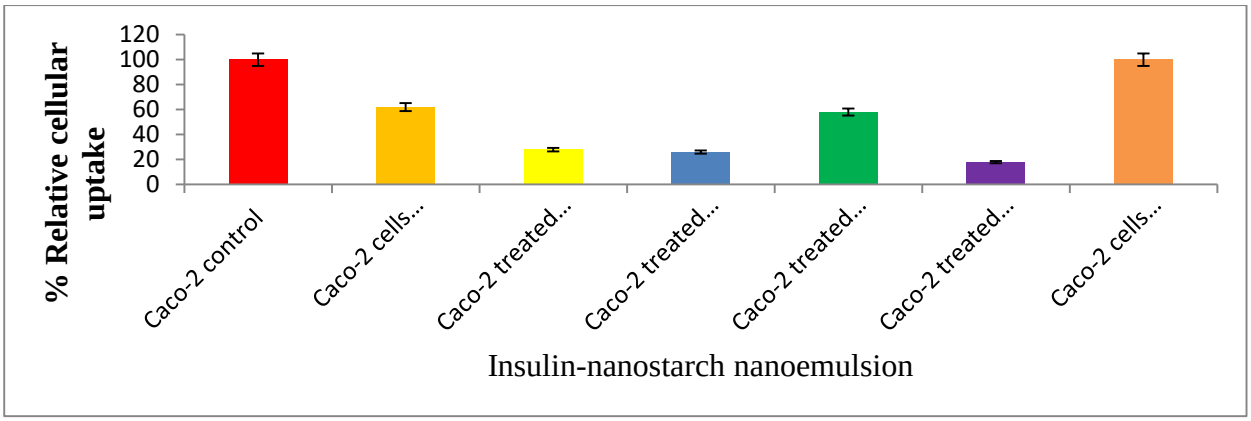

Graph 7 The effect of various endocytosis inhibitors on Caco-2 cellular insulin uptake after incubation with a nanostarch-insulin nanoemulsion

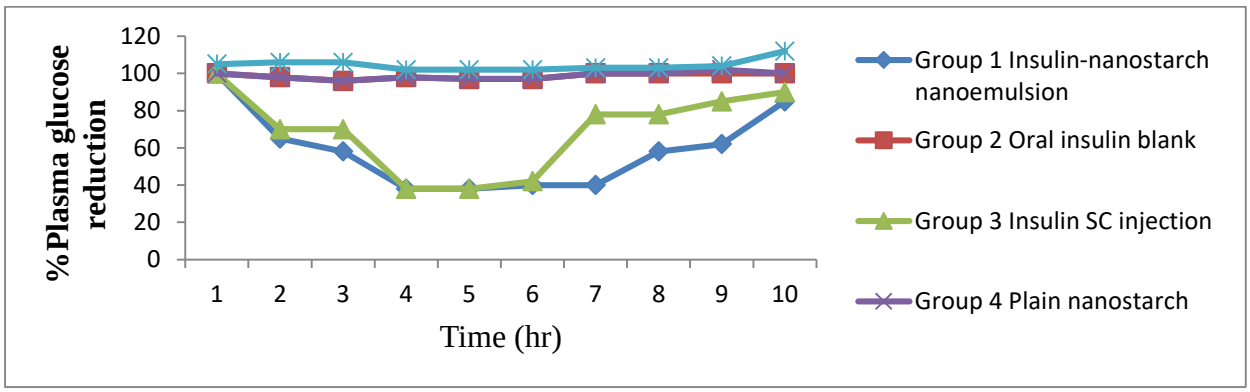

Graph. 8 (%) drop in plasma glucose after treatment

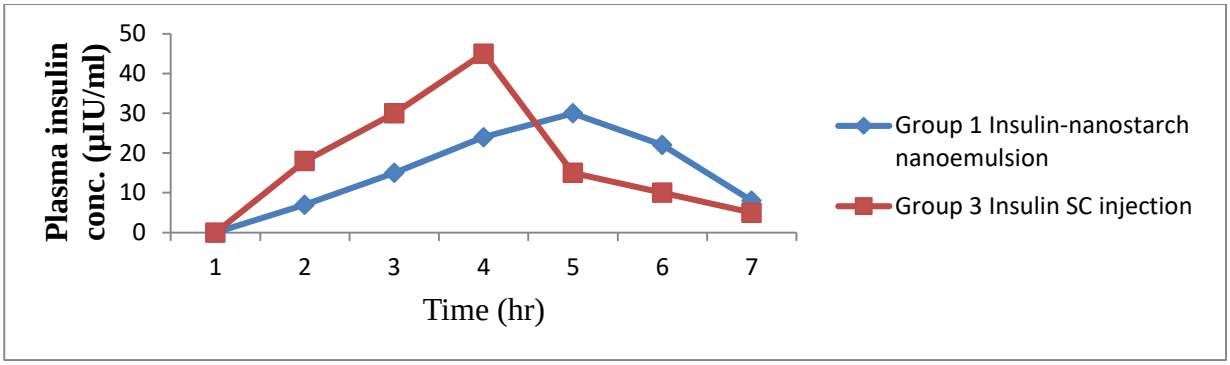

Graph. 9 Plasma insulin concentrations after oral insulin-nanostarch and sc injection

Table 2 Pharmacodynamics of oral nanostarch-insulin, sc insulin delivery

Groups	Initial plasma glucose conc. mg/dL)±SE	Pharmacodynamics parameters ± SE				
		Cmin (mg/dL)	Tmin (hr)	AUEC0-∞ (mg h/dL)	Total decrease in p.glu	(%)
Group 1 received oral nanostarch-Insulin*	259.83±5.32	118.66±8.38	6hr	1690.11±3.47	32.41±2.74	
Group 3 received insulin sc injection**	255.83±4.98	91.33±4.24	4hr	1814.59±3.24	27.45±2.55	

Table 3 Pharmacokinetics - after oral nanostarch-insulin treatment, sc insulin

Groups	Pharmacodynamics parameters ± SE				
	C_{max} (µIU/mL)	T_{max} (h)	AUC0-∞ (µIU h/mL)	MRT (h)	Relative bioavailability
Group 1 oral nanostarch-Insulin*	31.04±1.11	6hr	502.67±15.74	13.28±1.02	17.04%±1.34
Group 3 received insulin sc injection**	43.91±2.06	4hr	294.61±19.67	8.10±0.32	100

Results are the mean of six replicate±SE. *Insulin dose 50 IU/Kg. **Insulin dose 5 IU/Kg.

7.11 Intestinal uptake

The rat intestinal mucosa demonstrated no histological alterations following oral administration of the nanostarch-insulin nanoemulsion, confirming histocompatibility. There was no fluorescence in any section of the colon after taking insulin-FITC solution orally (Figs. 4a,b,c). This could be because insulin degrades rapidly in the gastrointestinal tract and cannot get through intestinal walls. In contrast, fluorescence was observed throughout the digestive tract. A nanostarch-insulin nanoemulsion, as previously shown, may protect insulin against enzymatic breakdown in the gastrointestinal system. Surprisingly, the nanoemulsion was discovered deep within the submucosa, muscular tissues, and the mucosal surface.

The electrostatic interaction between the positively charged nanoemulsion and the negatively charged cell membrane caused the nanoemulsion to adhere to the mucosa. Additionally, a nanostarch-insulin nanoemulsion was found in the Peyer patches. Previous research found that nanoemulsion internalisation in Peyer's patches was predominantly accomplished through adsorptive endocytosis. The ultimate features of nanostarch, such as mucoadhesion and penetration augmentation through the opening of cellular tight junctions, enable the nanoemulsion to enter the intestinal wall. These findings showed that the paracellular pathway involved both transcellular and receptor-mediated endocytosis [26]. These findings are compatible with the results of the cellular absorption process.

7.12 *In-vivo* pharmacodynamics and pharmacokinetic studies

The plasma % glucose reduction following oral administration of insulin solution and plain nanostarch-insulin nanoemulsion was comparable to that after oral PBS, showing that there was no hypoglycemic effect (Graphs 7,8,&9). As previously indicated, oral administration of insulin solution is sensitive to stomach enzymatic harshness, resulting in decreased intestinal absorption. In comparison to the control group, insulin-Nanostarch nanoemulsion and insulin subcutaneous injection dramatically lowered plasma glucose levels ($p<0.05$). Subcutaneous insulin infusion caused a significant decline in plasma glucose levels until 4 hours after hypoglycemia shock, when they returned to normal within 12 hours. After 6 hours (T_{min}) of oral administration of insulin-nanostarch nanoemulsion, plasma glucose levels dramatically fell from 259.83±5.32 to 118.66±8.38 mg/dL (C_{min}) ($p <0.05$) and recovered to normal within 24 hours. These findings support the nanoemulsion's delayed and long-lasting hypoglycemic effect. The AUEC-∞ after oral treatment with nanostarch-insulin nanoemulsion was 1690.11±3.47 mg/dL, resulting in a total reduction in plasma glucose levels of 32.41±2.74%, compared to 27.45±2.55% with subcutaneous injection (Table 2). Subcutaneous insulin injection significantly increased blood insulin concentrations to a maximum (C_{max}) of 43.90±2.06 µIU/mL after 4 hours (T_{max}), indicating optimal hypoglycemic activity (Fig. 5B, Table 3). Following that, serum insulin levels plummeted dramatically. In contrast, insulin-Nanostarch nanoemulsion absorption was slower, with a T_{max} of 6 hours, although blood insulin levels remained high for 24 hours (Fig. 5B). Rats given nanostarch-insulin nanoemulsion had a calculated $AUC0_{-\infty}$ of 502.67±15.74 µIU h/mL, indicating a 17.04±1.34% relative bioavailability (Table 3). Finally, the MRT of oral nanostarch-insulin nanoemulsion was substantially greater than that of subcutaneous insulin injection. Improving insulin intestinal permeability is an easy way to boost oral insulin bioavailability [27-30]. The increased cellular and intestinal absorption, as well as biological activity, of the generated nanoemulsion can be attributed to the nanoemulsion size and final component qualities. Nanoemulsions are suitable for mucosal uptake due to their small size. Improving nanoemulsion absorption in the gastrointestinal tract by targeting the colon's many vitamin B_{12} and folate receptors. The biodegradable nanostarch-insulin nanoemulsion interacts electrostatically with negatively charged cell membranes, allowing nanocargo into the cell [31-33]. Mucoadhesive characteristics are also connected to nanostarch's hydroxyl groups through hydrogen bonding and the hydrophobic contact between mucin and nanostarch [34-40].

Two frequently mentioned strategies include physical entanglement of polymer and mucus glycoproteins and increased hydration of OH-carrying matrices for faster diffusion across the intestinal mucosal layer. These connections aided nanoemulsion transcellular and paracellular internalisation [41-48].

8. Conclusion

The current work investigated the feasibility of creating an oral insulin formulation that combines the advantages of nanoencapsulation with lipid emulsion. Protein-stabilized nanoemulsions were found to be significantly more stable than surfactant, emulsifier, and cosurfactant-stabilised nanoemulsions. The emulsification / electrostatic self assembly cross linking technology were greatly improved to address the method's drawbacks, such as high size dispersion in the microscale and low recovery yield. These results demonstrated that employing ultrasonication to reduce the size of emulsion droplets and so make nanoscale particles was an efficient strategy. This procedure was improved by introducing the cosurfactant span 20. As a result, the previous discovery was likely due to enhanced protein surface potential. The process was simple and did not use any organic chemicals. In simulated stomach, intestinal, and PBS media, a nanostarch-insulin nanoemulsion effectively sustained insulin. Furthermore, gravity separation resistance and biocompatibility in nanostarch-insulin stabilised nanoemulsions were enhanced. Protein concentration, pH, and homogenization pressure all affect particle size, stability, transmission electron microscopy, morphology, and zeta potential. As a result, we believe that by combining insulin with proteins as a drug delivery model and castor oil as a surfactant, we can develop biocompatible and biodegradable nanoemulsion systems that can replace present surfactants. This functional nanoemulsion for oral delivery combines peptides, nucleotides, and hydrophilic large molecules. The CD-tested secondary structure of insulin demonstrated that it maintained biological activity during the encapsulation procedure. This electrostatic self-assembled optimised w/o/w nanoemulsion can enter monolayer Caco-2 cells through both paracellular and intracellular channels. Our preliminary cell culture results, as well as the ex vivo research, are quite promising. The TEER of nanoemulsion encapsulated with insulin is significantly lower than that of nanostarch, showing substantial tight-junction opening properties for this newly synthesised peptide-conjugated derivative of nanostarch. The coated nanoemulsion reduced glucose levels in diabetic mice by up to 61% and 51%, respectively, compared to their basal glucose levels at insulin dosages of 25 and 50 IU/kg, while insulin bioavailability was 8.19% and 7.84%, indicating good insulin intestinal absorption. These findings suggest that a nanostarch-insulin coated nanoemulsion could be developed as an oral therapeutic protein delivery system. In contrast, the biological activity of released insulin from nanoparticles after subcutaneous injection into diabetic male albino wistar rats demonstrated that insulin function was sustained. Insulin entrapped in nanoemulsion demonstrated a smaller and less severe decline than insulin released from nanoemulsion due to its interaction with polysaccharides. This optimised methodology, which used mild insulin encapsulation conditions and simple procedures, enabled the development of nanostarch-based insulin-loaded nanoemulsions with insulin activity retention in the nanometric range, which will have important applications in the pharmaceutical field in the future.

References

1. Wong CY., Al-Salami, H., Dass, C.R.,. "Potential of insulin nanoparticle formulations for oral delivery and diabetes treatment". *J. Control. Release*, 264 (2017): 247-275.
2. Su, F.Y., Lin, K.J., Sonaje, K., Wey, S.P., Yen, T.C., Ho, Y.C., et al. "Protease inhibition and absorption enhancement by functional nanoparticles for effective oral insulin delivery". *Biomaterials*, 33 (2012): 2801-2811.
3. Czuba, E., Diop, M., Mura, C., Schaschkow, A., Langlois, A., Bietiger, W., Neidl, R., Virciglio, A., Auberval, N., Julien-David, D., Maillard, E., Frere, Y., Marchioni, E., Pinget, M., Sigrist, S., et al. "Oral insulin delivery, the challenge to increase insulin bioavailability: influence of surface charge in nanoparticle system". *Int. J. Pharm*, 542 (2018): 47-55.
4. Angellier, H., Choisnard, L., Molina-Boisseau, S., Ozil, P., Dufresne, A., "Optimization of the preparation of aqueous suspensions of waxy maize starch nanocrystals using a response surface methodology", *Biomacromolecules*, 5(4) (2004): 1545-1551.
5. Salatin, S., Khosroushahi, Y.A., "Overviews on the cellular uptake mechanism of polysaccharide colloidal nanoparticles". *J. Cell Mol. Med*, 21(2017): 1668-1686.
6. Fan, W., Xia, D., Zhu, Q., Li, X., He, S., Zhu, C., Guo, S., Hovgaard, L., Yang, M., Gan, Y., et al. "Functional nanoparticles exploit the bile acid pathway to overcome multiple barriers of the intestinal epithelium for oral insulin delivery". *Biomaterials*, 151(2018): 13-23.
7. Gedawy, A., Martinez, J., Al-Salami, H., Dass, C.R., "Oral insulin delivery: existing barriers and current counter-strategies". *J. Pharm. Pharmacol*, 70 (2018): 197-213.
8. Grant, J., Lee, H., Liu, R.C., Allen, C., "Intermolecular interactions and morphology of aqueous polymer/surfactant mixtures containing cationic chitosan and nonionic sorbitan esters". *Biomacromolecules*, 9 (2008): 2146-2152.
9. Roger, E., Kalscheuer, S., Kirtane, A., Guru, B.R., Grill, A.E., Whittum-Hudson, J., Panyam, J., et al. "Folic acid functionalized nanoparticles for enhanced oral drug delivery". *Mol. Pharm*, 9 (2012): 2103-2110.
10. Illum, L., "Nanoparticulate systems for nasal delivery of drugs: a real improvement over simple systems". *J. Pharm. Sci*, 96 (2007): 473-483.
11. Tian, H., He, Z., Sun, C., Yang, C., Zhao, P., Liu, L., et al. "Uniform core-shell nanoparticles with thiolated hyaluronic acid coating to enhance oral delivery of insulin". *Adv. Healthc. Mater*, 7 (2018): e1800285.
12. Wang, L., Zhang, J., Song, M., Tian, B., Li, K., Liang, Y., Han, J., Wu, Z., et al. "A shell cross linked polymeric micelle system for pH/redox dual stimuli-triggered DOX on-demand release and enhanced antitumor activity". *Colloids Surf. B, Biointerf*, 152 (2017): 1-11.
13. Di Marzio, L., Marianecci, C., Cinque, B., Nazzarri, M., Cimini, A.M., Cristiano, L., Cifone, M.G., Alhaique, F., Carafa, M., et al. "pH-sensitive non-phospholipid vesicle and macrophage-like cells: binding, uptake and endocytotic pathway". *Biochim. Biophys. Acta*, 1778 (2008): 2749-2756.
14. Zhao, F., Zhao, Y., Liu, Y., Chang, X., Chen, C., Zhao, Y., et al. "Cellular uptake, intracellular trafficking, and cytotoxicity of nanomaterials". *Small*, 7(2011a): 1322-1337.

15. Elmowafy, E., Osman, R., El-Shamy, A.H., Awad, G.A., "Nanocomplexes of an insulinotropic drug: optimization, microparticle formation, and antidiabetic activity in rats". *Int. J. Nanomed,* 9 (2014): 4449-4465.
16. Huang, Y., Leobandung, W., Foss, A., Peppas, N.A., "Molecular aspects of muco and bioadhesion: tethered structures and site-specific structures". *J. Control. Release,* 65 (2000): 63-71.
17. Su, F.Y., Lin, K.J., Sonaje, K., Wey, S.P., Yen, T.C., Ho, Y.C., et al. "Protease inhibition and absorption enhancement by functional nanoparticles for effective oral insulin delivery". *Biomaterials,* 33 (2012): 2801-2811.
18. Tian, H., He, Z., Sun, C., Yang, C., Zhao, P., Liu, L., et al. "Uniform core-shell nanoparticles with thiolated hyaluronic acid coating to enhance oral delivery of insulin". *Adv. Healthc. Mater,* 7 (2018): e1800285.
19. Wang, L., Zhang, J., Song, M., Tian, B., Li, K., Liang, Y., Han, J., Wu, Z., et al. "A shell cross linked polymeric micelle system for pH/redox dual stimuli-triggered DOX on-demand release and enhanced antitumor activity". *Colloids Surf. B, Biointerf,* 152 (2017): 1-11.
20. Illum, L., "Nanoparticulate systems for nasal delivery of drugs: a real improvement over simple systems". *J. Pharm. Sci,* 96 (2007): 473-483.
21. Jain, S., Rathi, V.V., Jain, A.K., Das, M., Godugu, C., "Folate-decorated PLGA nanoparticles as a rationally designed vehicle for the oral delivery of insulin". *Nanomedicine,* 7 (2012): 1311-1337.
22. Yu, J., Zhang, Y., Bomba, H., Gu, Z., "Stimuli-responsive delivery of therapeutics for diabetes treatment". *Bioeng. Transl. Med,* 1 (2016): 323-337.
23. Zhang, H., Yamazaki, T., Zhi, C., Hanagata, N., "Identification of a boron nitride nanosphere-binding peptide for the intracellular delivery of CpGoligodeoxynucleotides". *Nanoscale,* 4 (2012): 6343-6350.
24. Mukherjee, S., Ray, S., Thakur, R.S., "Design and evaluation of itraconazole loaded solid lipid nanoparticulate system for improving the antifungal therapy". *Pakistan J. Pharm. Sci,* 22 (2009): 131-138.
25. Dyawanapelly, S., Koli, U., Dharamdasani, V., Jain, R., Dandekar, P., "Improved mucoadhesion and cell uptake of chitosan and chitosan oligosaccharide surface modified polymer nanoparticles for mucosal delivery of proteins". *Drug Deliv. Trans. Res,* b (2016): 365-379.
26. El-Leithy, E.S., Abdel-Bar, H.M., Abd el-Moneum, R., "Synthesis, optimization and characterization of folate-chitosan polymer conjugate for possible oral delivery of macromolecular drugs". *IOSR J. Pharm,* 7 (2017): 30-38.
27. Elmowafy, E., Osman, R., El-Shamy, A.H., Awad, G.A., "Nanocomplexes of an insulinotropic drug: optimization, microparticle formation, and antidiabetic activity in rats". *Int. J. Nanomed,* 9 (2014): 4449-4465.
28. Parmar, H.S., Kar, A., "Protective role of *Mangifera indica, Cucumis melo* and *Citrullus vulgaris* peel extracts in chemically induced hypothyroidism". *Chem. Biol. Interact,* 177 (2009): 254-258.
29. Rahbarian, M., Mortazavian, E., Dorkoosh, F.A., Tehrani, M.R., "Preparation, evaluation and optimization of nanoparticles composed of thiolatedtriethyl chitosan: a potential approach for buccal delivery of insulin". *J. Drug Delivery Sci. Technol,* 44 (2018): 254-263.

30. Ooya, T., Eguchi, M., Ozaki, A., Yui, N., "Carboxyethylester-polyrotaxanes as a new calcium chelating polymer: synthesis, calcium binding and mechanism of trypsin inhibition". *Int. J. Pharm*, 242 (2002): 47-54.
31. Kriwet, B., Kissel, T., "Interactions between bioadhesive poly(acrylic acid) and calcium Ions". *Int. J. Pharm*, 127 (1996): 135-145.
32. Li, P., Wang, Y., Zeng, F., Chen, L., Peng, Z., Kong, L.X., et al. "Synthesis and characterization of folate conjugated chitosan and cellular uptake of its nanoparticles in HT-29 cells". *Carbohydr. Res*, 346 (2011): 801-806.
33. Ahmed, T.A., Aljaeid, B.M., "Preparation, characterization, and potential application of chitosan, chitosan derivatives, and chitosan metal nanoparticles in pharmaceutical drug delivery". *Drug Des., Dev. Therapy*, 10 (2016): 483-507.
34. Aiedeh, K., Tahab, M.O., "Synthesis of chitosan succinate and chitosan phthalate and their evaluation as suggested matrices in orally administered, colon-specific drug delivery systems". *Arch. Pharm*, 332 (1999): 103-107.
35. Benavent, A.F.R., Perera, N.Y., Alonso, D.F., Perea, S.E., Gomez, D.E., Farina, H.G., et al. "Mechanisms of cellular uptake, intracellular transportation, and degradation of CIGB-300, a Tat-conjugated peptide, in tumor cell lines". *Mol. Pharm*, 11 (2014): 1798-1807.
36. Calvo, P., Remuñan-Lopez, C., Vila-Jato, J.L., Alonso, M.J., "Novel hydrophilic chitosan-polyethylene oxide nanoparticles as protein carriers". *J. Appl. Polym. Sci*, 63 (1997): 125-132.
37. Liu, M., Zhong, X., Yanga, Z., "Chitosan functionalized nanocochleates for enhanced oral absorption of cyclosporine". *A. Sci. Rep*, 7 (2017): 41322.
38. Luippold, G., Bedenik, J., Voigt, A., Grempler, R., "Short and long term glycemic control of streptozotocin-induced diabetic rats using different insulin preparations". *PLoS ONE* 11 (2016): e0156346.
39. Mellman, I., Nelson, W.J., 2008. "Coordinated protein sorting, targeting and distribution in polarized cells". *Nat. Rev. Mol. Cell Biol*, 9 (2008): 833-845.
40. Rahbarian, M., Mortazavian, E., Dorkoosh, F.A., Tehrani, M.R., "Preparation, evaluation and optimization of nanoparticles composed of thiolatedtriethyl chitosan: a potential approach for buccal delivery of insulin". *J. Drug Delivery Sci. Technol*, 44 (2018): 254-263.
41. Rathnam, G., Balasubramani, P., Saravanakumar, A., "Nasal drug delivery of antidiabetic drug repaglinide using degradable starch microspheres". *Int. J. Pharm. Sci. Res*, 2, 940-947 (2011)
42. Abdel-Bar, H.M., El Basset, S.R.A., "Endocytic pathways of optimized resveratrol cubosomes capturing into human hepatoma cells". *Biomed. Pharmacother*, 93 (2017): 561-569.
43. Agrawal, A.K., Harde, H., Thanki, K., Jain, S., "Improved stability and antidiabetic potential of insulin containing folic acid functionalized polymer stabilized multi layered liposomes following oral administration". *Biomacromolecules*, 15 (2014): 350-360.
44. Agrawal, A.K., Urimi, D., Harde, H., Kushwah, V., Jain, S., "Folate appended chitosan nanoparticles augment the stability, bioavailability and efficacy of insulin in diabetic rats following oral administration". *Royal Soc. Chem. Adv*, 5 (2015): 105179-105193.

45. Ahmed, T.A., Aljaeid, B.M., “Preparation, characterization, and potential application of chitosan, chitosan derivatives, and chitosan metal nanoparticles in pharmaceutical drug delivery”. *Drug Des., Dev. Therapy,* 10 (2016): 483-507.
46. Di Marzio, L., Marianecci, C., Cinque, B., Nazzarri, M., Cimini, A.M., Cristiano, L., Cifone, M.G., Alhaique, F., Carafa, M., et al. “pH-sensitive non-phospholipid vesicle and macrophage-like cells: binding, uptake and endocytotic pathway”. *Biochim. Biophys. Acta*, 1778 (2008): 2749-2756.
47. Hsu, L.W., Lee, P.L., Chen, C.T., Mi, F.L., Juang, J.H., Hwang, S.M., Ho, Y.C., Sung, H.W., et al. “Elucidating the signaling mechanism of an epithelial tight-junction opening induced by chitosan”. *Biomaterials,* 33 (2012): 6254-6263.
48. Huang, Y., Leobandung, W., Foss, A., Peppas, N.A., “Molecular aspects of muco and bioadhesion: tethered structures and site-specific structures”. *J. Control. Release,* 65 (2000): 63-71.